Supporting Information

Controlled HCl Etching of Al_2O_3 Nanoparticles toward Void-Free Interfacial Contact for Efficient Perovskite Solar Cells

Yi Wang[a], Qiangqiang Zhao[b], Bingqian Zhang[b], Panyu Wang[b], Nannan Gao[b], Kun Gao[b], Qi Huang[b,*], Xiaojie Song[a,*] and Shuping Pang[b,*]

[a] School of Materials Science and Engineering, Shandong University of Science and Technology, Qingdao, 266590, China

[b]State Key Laboratory of Photoelectric Conversion and Utilization of Solar Energy, Qingdao New Energy Shandong Laboratory, Qingdao Institute of Bioenergy and Bioprocess Technology, Chinese Academy of Sciences, Qingdao 266101, P.R. China

Materials:

Mix anhydrous $SnCl_4$ and deionized water in a volume ratio of 1:75 to obtain a precursor solution of SnO_2. The obtained solution is aged for two weeks at a temperature of 25 ℃, and the solution changes from a clear and transparent solution to a white colloidal solution. Lead iodide (PbI_2) was purchased from Advanced Electron Technology. Formamidinium iodide (FAI), cesium iodide (CsI) were purchased from Xi'an Polymer Light Technology Corp in China. N, N-dimethylformamide (DMF), dimethyl sulfoxide (DMSO), 4-tert-butylpyridine (tBP) and lithium bis (trifluoro-methanesul-fonyl) imide (Li-TFSI) were purchased from Sigma Aldrich. Spiro-OMeTAD were purchased from BORUN NEW MATERIAL TECHNOLOGY LIMITED. Nano Al_2O_3 alcohol dispersion, 30 nm particle size, 20 wt.% alcohol solution was purchased from Preferred Technology Co., Ltd. Hydrochloric acid (HCl, analytical grade, 12 mol/L) was purchased from Sinopharm Chemical Reagent Co., Ltd. The above chemicals were used as received without any purification.

Device fabrication:

Fluorine doped tin oxide (FTO) coated glass is sequentially cleaned with detergent once, deionized water once, and anhydrous ethanol twice, each time for 30 minutes of ultrasonic cleaning. Blow dry the cleaned FTO glass for later use. A dense TiO_2 layer was deposited by atomic layer deposition (ALD) and annealed at 500 for 30 minutes. The prepared SnO_2 was spin coated on FTO/TiO_2 glass at 3000rpm for 30 seconds, and then annealed at 180 ℃ for 30 minutes to obtain a SnO_2 electron transport layer. The HCl-treated Al_2O_3 colloidal solutions were prepared as follows. First, 10 μL of commercial Al_2O_3 paste was diluted 150-fold with isopropanol to a final volume of 1.5 mL. Separately, concentrated HCl (12mol/L) was diluted 100-fold with deionized water. Then, 9.7 μL of the diluted HCl solution was added to the as-prepared Al_2O_3 dispersion (1.5 mL). The amount of HCl added was calculated to be capable of etching up to 1 mol% of the Al_2O_3 present (denoted as 1% A-Al_2O_3). The mixture was sonicated in an ultrasonic bath for 1 h. Solutions targeting other etching capacities (e.g., 2%, 4%, 8% of the Al_2O_3) were prepared analogously by adjusting the

concentration of the diluted HCl solution while keeping the total volume constant. The resulting mixtures were stored in appropriate containers. Diluted Al2O3 dispersion was spin coated on the SnO_2 electron transport layer at a speed of 5000rpm for 30s. After spin-coating, the films are annealed at 100 ℃ for 30s on a hot bench in air.

To prepare a 1.4 M $FA_{0.95}Cs_{0.05}PbI_3$ precursor solution, 228.8 mg of FAI, 18.2 mg of CsI, and 645.4 mg of PbI_2 were dissolved in a mixed solvent of 800 µL DMF and 200 µL DMSO. Spin the perovskite solution at 1000 rpm for 10 seconds, then spin it at 4000 rpm for 30 seconds. In the last 10 seconds of the second step, drop 300ul of anisole at a constant rate at the center of FTO. After spin-coating, the perovskite films are first annealed at 140 ℃ for 30s on a hot bench in a glove box and then transferred to air environment with humidity less than 30% at 150 ℃ for annealing for 20 min. The Spiro-OMeTAD hole-transporting layer (HTL) was prepared by mixing Spiro-OMeTAD (72.3 mg), 4-tert-butylpyridine (28.8 µL) and of Li-TSFI (17.5 µL) solution (520 mg Li-TSFI in 1 mL acetonitrile) in chlorobenzene (1 mL). The prepared Spiro-OMeTAD solution was spin coated on the perovskite film at a speed of 3000rpm for 30 seconds to obtain a Spiro-OMeTAD hole transport layer. Finally, age the prepared device in a drying air box for 24 hours. Use a vacuum evaporation device to thermally evaporate an 80 nm thick Au electrode under vacuum at a rate of 0.5-1.0 Å/s.

The fabrication procedure for the 50 × 50 mm^2 module is as follows: First, FTO substrates were cleaned following the same procedure used for small-area devices. Subsequently, P1 laser scribing was performed to pattern the FTO layer. After scribing, the substrates were cleaned by ultrasonic treatment twice with anhydrous ethanol. A compact TiO_2 layer was then deposited by atomic layer deposition (ALD) and annealed at 500 ℃ for 30 min. The subsequent deposition steps were identical to those used for small-area devices, yielding the full stack of FTO/TiO_2/SnO_2/A-Al_2O_3/$FA_{0.95}Cs_{0.05}PbI_3$/spiro-OMeTAD. The completed devices were stored in a dry air box for 48 h for aging. Finally, P2 laser scribing was applied to expose the conductive bottom electrode, followed by thermal evaporation of an 80 nm gold electrode. P3 laser scribing was then performed to isolate the individual sub-cells, with a 5 mm margin at the top and bottom edges to ensure insulation.

Characterization

XRD patterns were measured by a Bruker-AXS Micro diffractometer (D8 ADVANCE) with Cu Kα radiation (1.5406Å). The optical absorbance spectra were measured by UV-vis/NIR spectrophotometer (U-4100, Hitachi). Steady Photoluminescence (PL) spectra were recorded on a Perkin LS-55 fluorescence spectrometer excited at 450 nm. For TRPL measurements, the data were acquired using a transient fluorescence lifetime imaging spectrometer (Nanolog, HORIBA, USA) with an excitation wavelength of 438 nm and a monitoring wavelength of 780 nm, with the films excited from the perovskite side. For DLS measurements, the hydrodynamic size distribution of Al_2O_3 nanoparticles was characterized using a nanoparticle size analyzer (Zetasizer Ultra, Malvern Panalytical, UK) at room temperature. To ensure accuracy, the dispersions were successively diluted until stable readings were obtained, minimizing scattering effects from high concentrations. The planar and cross-sectional SEM images were obtained through field emission scanning electron microscopy (S-4800, Hitachi). The X-ray exposure of the sample was only 15 min during the

measurement. The P1-P2-P3 process involves the precise etching of large components, utilizes the Pulsed Laser & Green Light Picosecond Dual-Path Technology (Suzhou Microtreat Intelligent Technology Co., Ltd). J-V curves of the as-fabricated PSCs with different scanning directions were measured using a 2400 Sourcemeter (Keithley, USA) under simulated 1-sun AM 1.5G 100 mW cm^{-2} intensity (Oriel Sol3A Class AAA, Newport, USA). The typical active area of PSCs is 0.09 cm^2 defined by a metal mask. The intensity of the 1-sun AM 1.5G illumination was calibrated using a Si-reference cell certified by the National Renewable Energy Laboratory. The External Quantum Efficiency (EQE) measurement was calculated using certified incident photon to current conversion efficiency equipment from Enlitech (Taiwan).

For the stability tests, all PSCs were without encapsulation. The operational stability was performed using a stability setup (LC Auto-Test 24, Shenzhen Lancheng Technology Co., Ltd.), tested under continuous light illumination and maximum power point tracking (controlled and monitored to be 20℃). The light source consisted of an array of white LEDs powered by a constant current. The LED type is MG-A200A-AE with an emission spectrum of 400-750 nm. Equivalent sun intensities were calibrated using a calibrated Si-reference cell. During aging, the device is connected with a 100 Ohm load resistance. To comprehensively assess device robustness, unencapsulated cells were subjected to continuous maximum-power-point tracking under 1-sun illumination (no UV filter) in an inert (N_2) atmosphere, with performance data recorded every 6 hours throughout the test.

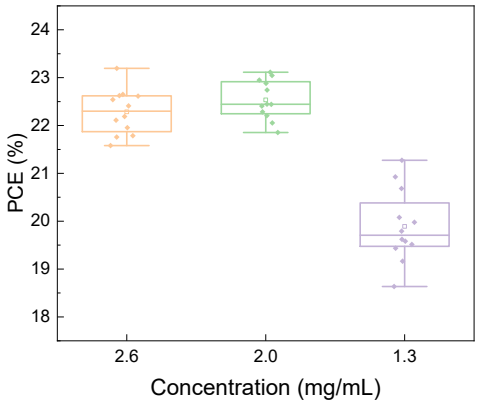

Figure S1. Photovoltaic performance of devices with varying concentrations of C-Al_2O_3. Statistical distribution of the power conversion efficiency (PCE) for solar cells fabricated with different concentrations of C-Al_2O_3 nanoparticles in the interlayer.

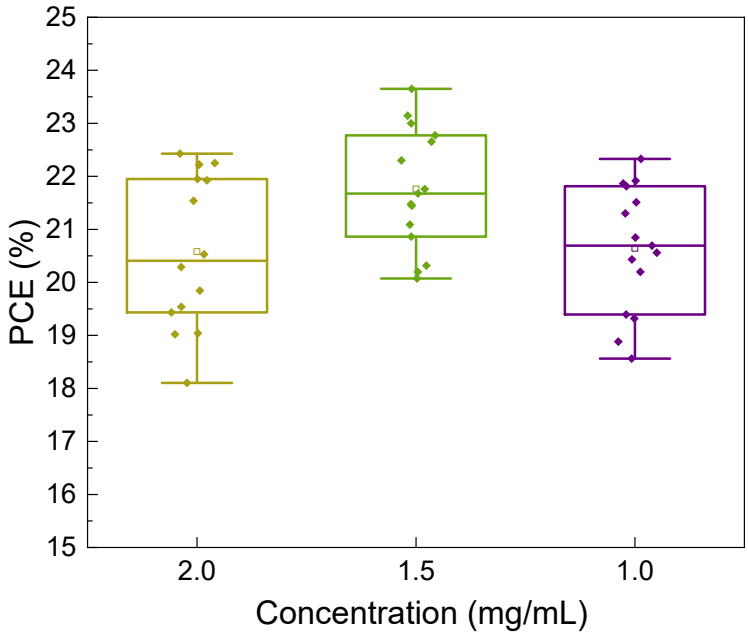

Figure S2. Photovoltaic performance of devices with varying concentrations of A-Al_2O_3. Statistical distribution of the power conversion efficiency (PCE) for perovskite solar cells fabricated using different concentrations of A-Al_2O_3 nanoparticles.

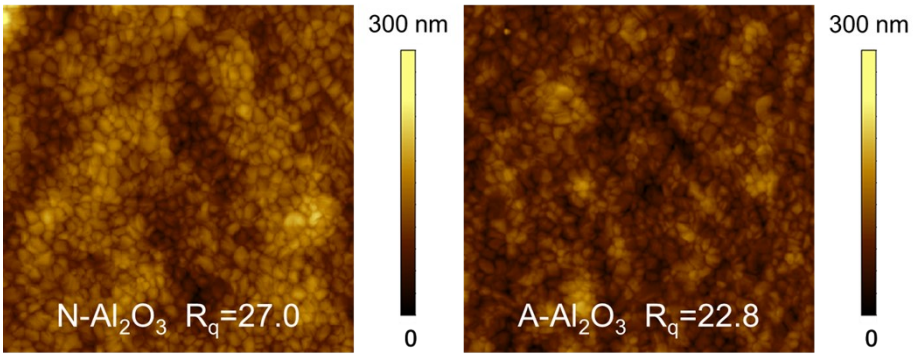

Figure S3. Surface roughness comparison of perovskite films. Atomic force microscopy (AFM) images and corresponding root-mean-square (RMS) roughness values (in nm) of perovskite films deposited on substrates with N-Al_2O_3 or with A-Al_2O_3;

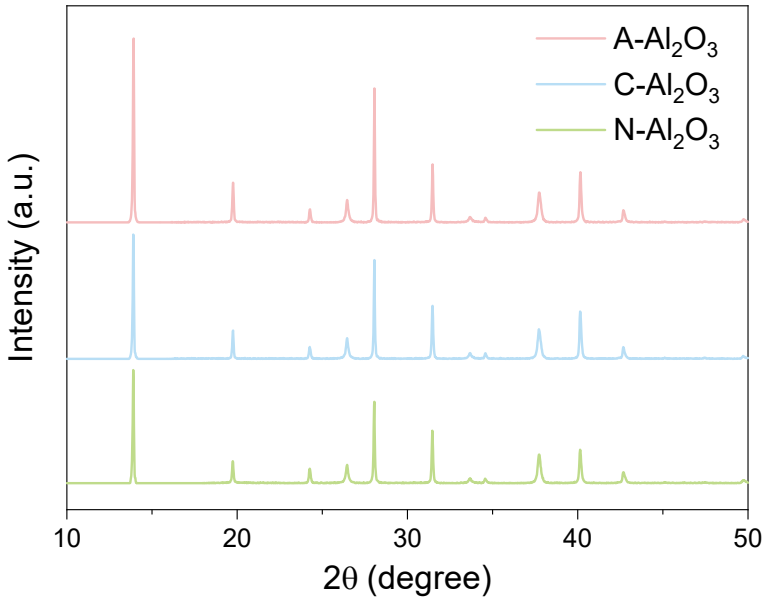

Figure S4. X-ray diffraction (XRD) patterns of perovskite films with different Al_2O_3 treatments. Comparison of XRD patterns for perovskite films prepared with N-Al_2O_3, with C-Al_2O_3, and with A-Al_2O_3. The measurements were performed with excitation at 438 nm and monitored at 780 nm, with the films excited from the perovskite side.

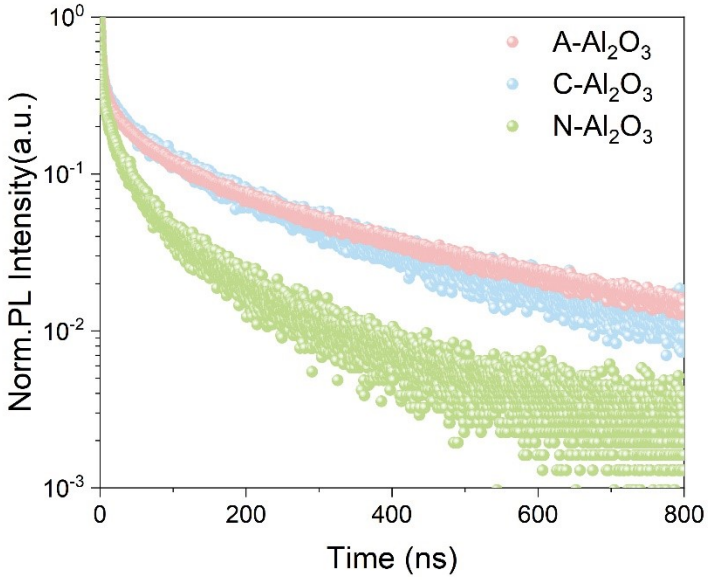

Figure S5. Time-resolved photoluminescence (TRPL) decay dynamics. Comparison of TRPL decay curves for perovskite films prepared with N-Al_2O_3, with C-Al_2O_3, and with A-Al_2O_3.

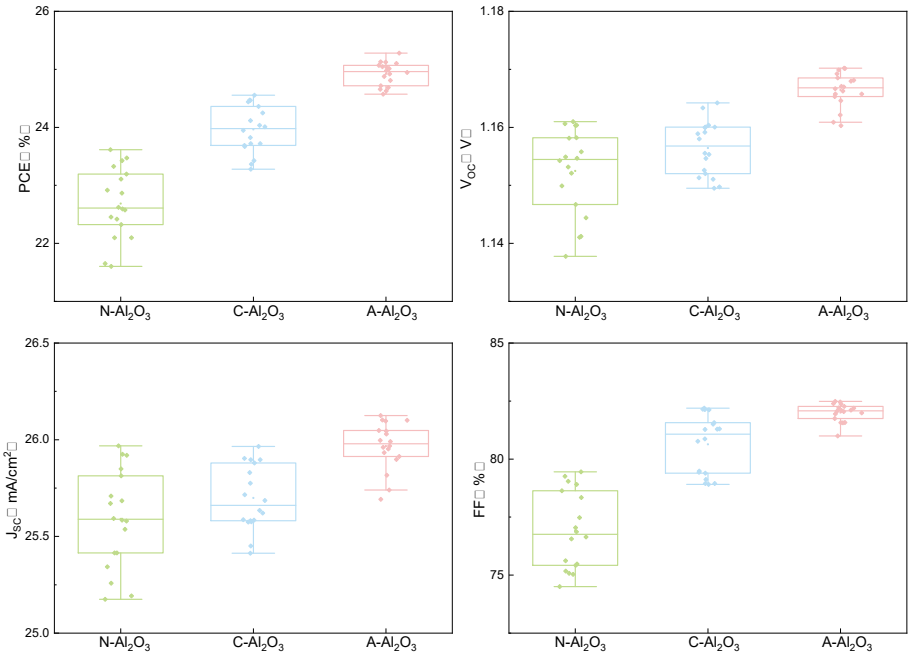

Figure S6. Statistical distribution of photovoltaic parameters for devices with different Al_2O_3 treatments. Histograms of (a) power conversion efficiency (PCE), (b) open-circuit voltage (VOC), (c) short-circuit current density (JSC), and (d) fill factor (FF) for perovskite solar cells prepared with N-Al_2O_3, with C-Al_2O_3, and with A-Al_2O_3.

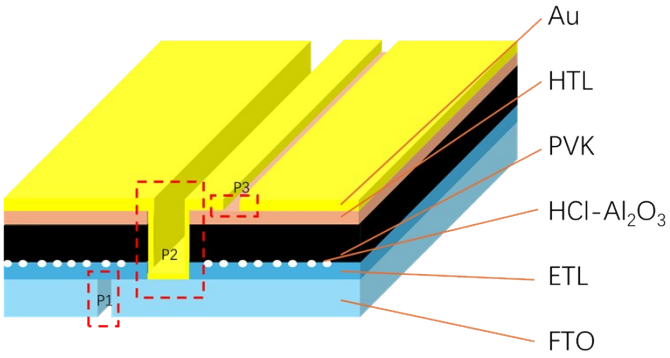

Figure S7. Schematic of the perovskite solar module structure. The diagram illustrates the layered architecture of the module, with the laser scribing lines (P1, P2, P3) outlined in red circles.

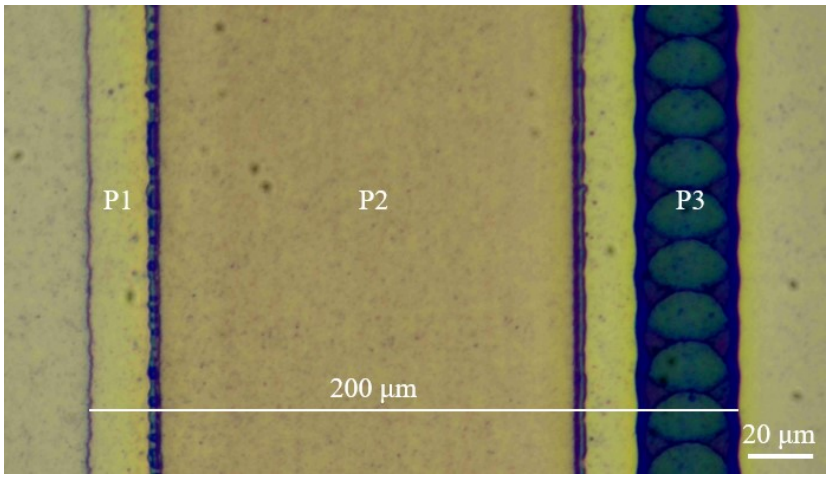

Figure S8. Schematic layout of the 50 × 50 mm^{2}perovskite solar module, highlighting the dead area width.

Table S1. Triexponential fitting parameters of TRPL decay curves for perovskite films with different Al2O3 treatments.

	N-Al2O3	C-Al2O3	A-Al2O3
A1	0.67837	0.58788	0.60867
τ 1 (s)	2.41E-09	3.43E-09	3.90E-09
A2	0.22857	0.2579	0.23053
τ 2 (s)	5.25E-08	1.23E-07	1.39E-07
τ avg (ns)	46.5	116	130